ISSN NO. 2320-5407

Journal homepage: http://www.journalijar.com

INTERNATIONAL JOURNAL OF ADVANCED RESEARCH

RESEARCH ARTICLE

Water Chemistry Effect on Corrosion of Nuclear Fuel Cladding Material, Zircaloy-4 (Zr-4)

Abdel–Hakim Kandil,[1] Abdel–Aziz Fahmy Waheed,[2] and Hani M. H. Tawfik[3*]

1. Professor of Nuclear and Inorganic Chemistry, Faculty of Science, Helwan University, Cairo, Egypt.
2. Professor of Metallurgy, Nuclear Metallurgical Department, Division of Materials, Nuclear Research Center, Egyptian Atomic Energy Authority (EAEA), Anshas, Egypt.
3. Post graduate Student, Chemistry Department, Faculty of Science, Zagazig University, Zagazig, Sharkia, Egypt.

Manuscript Info

Manuscript History:

Received: 12 February 2014
Final Accepted: 22 March 2014
Published Online: April 2014

Key words:
Nuclear fuel cladding materials, Zircaloy-4, lithium hydroxide (LiOH), boric acid (H_3BO_3), cyclic polarization technique, SEM.

***Corresponding Author**

Archana Sharma

Abstract

Effect of lithium and boron on waterside corrosion rate of the nuclear fuel cladding material, Zircaloy-4 (Zr-4), was measured through Tafel calculations using cyclic polarization technique at room temperature. In addition, passivity of ZrO_2 film was discussed through cyclic potentiodynamic polarization curves. After the corrosion experiments, the surface of the formed oxides were characterized by SEM. Lithium concentration in water covered the range 2.2 to 7000 ppm Li ions as lithium hydroxide (LiOH). At 100 ppm lithium in aqueous solution, boron added at 10 up to 4000 ppm as boric acid (H_3BO_3). Results showed that the corrosion of Zircaloy-4 is accelerated at high concentration of LiOH not in the diluted solutions. From the presented work, it is suggested that the enhancement of corrosion is caused by porosity generation through the oxide film. Below a critical LiOH concentration, only superficial porosity was developed in these short-duration experiments. At this critical concentration (which lies between 0.5 and 1.0 M LiOH for Zircaloy-4 at room temperature) porosity develop throughout the whole oxide layer and corrosion rates are enhanced. Boric acid has ameliorating effect on the degradation of Zircaloy-4 corrosion resistance caused by LiOH. PH effect and blocking mechanism can be proposed as inhibition mechanism.

Introduction

In Pressurized Water Reactors (PWRs), lithium is added as lithium hydroxide together with boric acid to the primary coolant. Boric acid (H_3BO_3) is added as chemical shim (Ramasubramanian and Balakrishnan, 1994) to control the core reactivity according to the nuclear reaction $^{10}B(n, \alpha)^7Li$. The alkali, lithium hydroxide (LiOH), is added to the primary coolant for PH control in order to control the corrosion of primary system materials and cladding, and minimize corrosion product transport within the primary system and thereby decreases the activation of out of core components (Ramasubramanian et al., 1989) and (Cheng et al., 1996).

Since the late 1970s, there has been a continuous demand to improve uranium utilization and reduce of nuclear fuel cycle cost. This will require extending fuel burnup by means of longer cycle operation, longer total in-reactor residence time, and higher heat rating (Cheng et al., 1996). For longer fuel cycle operations with higher target discharge burnups, the startup concentrations of boric acid, and thus lithium hydroxide, need to be increased (Cheng et al., 1996). However, the desire to increase fuel residence time and burnup will result in increased rates of corrosion of fuel cladding alloys (usually zirconium alloys, due to its corrosion resistance and low absorption cross section for neutron) in reactors (Bramwell et al., 1991) and may require removal of fuel before the end of its reactivity capability if maximum oxide thicknesses exceed some selected value such as 120 µm (Cheng et al., 1996).

In order to explain the accelerated corrosion of cladding in reactor, several hypotheses were proposed such as corrosion hydrogen precipitation (Kim et al., 2002), radiation effects in the oxide films (Garzarolli et al., Dec. 1982), metallurgical variables (tin and intermetallic particles) (Cheng et al., 1996), (Billot et al., 1994), and (Sabol, et al., 1994), ZrO_2 film thermal conductivity (oxide thicknesses effect) and thermal feedback (Cheng et al., 1996) and (Garzarolli et al., 1982), and primary coolant chemistry (lithium, boron, and oxygen content) (Billot et al., 1994), (Garzarolli et al., 1982), and (Sabol et al., April, 1994). Therefore, all must be considered, in interpreting high burnup oxide data.

It is known, from out-of-reactor tests, that in absence of boric acid, the corrosion of Zircaloy is accelerated in high temperature water or steam when LiOH is present in sufficient concentrations (more than LiOH concentration in PWRs). The argument for the possibility of an increase in rate of corrosion due to lithium in-reactor is based on: Depending on the thermo-hydraulic conditions at the wall of the fuel claddings, local boiling on the surface of or within a porous oxide or crud layer on fuel cladding may act as a concentrating mechanism and so raise the local lithium levels above those in the bulk coolant, this process known as hideout (Bramwell et al., 1991), (Billot et al., 1994), and (Pêcheur et al., 1996). Chemical concentration process which extracts water from the solution in the pores to form additional ZrO_2 also act as a concentration mechanism (Cox et al., 1996).

Different mechanisms describing the accelerated oxidation in the presence of lithium hydroxide: 1- Solid Solution Model: (Hillner and Chirigos, 1962). 2- Porosity Generation Model: (Ramasubramanian, 1991) and (Cox et al., 1996). 3- Crystal Growth Modification (Alteration) Mechanism (Garzarolli et al., 1991) and (Ramasubramanian and Balakrishnan, 1994). 4- Gradual Degradation of the Inner Barrier Layer (Pêcheur et al., 1996) and (Pêcheur et al., 2000).

The objective of this work is to study the electrochemical behaviour of fuel cladding alloy, namely Zircaloy-4, in presence of lithium ions (reported to be contributing to the accelerated corrosion of Z-4 in PWRs) and boron ions. For simple extrapolation of the relationship between the corrosion process and water chemistry (Li and B) the electrochemical corrosion tests were conducted at room temperature to eliminate the effect of high temperature and pressure on the electrochemical process.

Experimental Work

Cladding Material, Chemicals, and Preparation of Solution

The cladding material used in this study is Zircaloy-4 (Zr-4) was supplied by Nuclear Metallurgical Department. The main alloying elements in the cladding are shown in Table 1. Zircaloy-4 was received as tube; the tube was lengthwise cut, cold rolled and then cut into testing specimens. The specimens surfaces were polished with 6 micron diamond paste, subsequent cleaned in acetone/ethyl alcohol and then pickled in a solution of HF : HNO_3 : pure H_2O, and finally washed with deionized water and dried. The peripheral region of the specimen for electrochemical testing was covered with insulating resin; leaving an area of 0.5 cm^2. The preparation process for each specimen was directly conducted before each electrochemical test. Lithium hydroxide monohydrate ($LiOH.H_2O$) was manufactured by Loba Chemie, Mumbai, India and boric acid (H_3BO_3) was manufactured by Universal Fine Chemicals, India. Lithium hydroxide ($LiOH.H_2O$) and boric acid (H_3BO_3) were weighed using a balance Mettler Toledo, AG245. Pure deionized water is used for solutions preparation and refresh solution was directly prepared before each test.

Electrochemical Corrosion Tests and Oxide Surface Appearance

Anodic oxidation can be used to produce oxide films on zirconium alloys. Compared to autoclave testing it is possible to produce oxide films in short times (Oskarsson, 2000).

The equipment consisted of a potentiostate (EG&G Princeton Applied Research, Model 352/252 Corrosion Analysis Software, version 2.23), computer system, and an electrolysis cell. A two graphite electrodes and saturated calomel electrode (SCE) were used for the counter electrode and reference electrode, respectively.

The potentiostat described above was operated with cyclic potentiodtnamic polarization scan; initial delay (ID) 600 second, initial potential equal –0.1 versus open circuit potential (OC), vertex at 0.2 versus reference electrode potential, final potential at 0.1 versus reference electrode potential, and the scan rate of potential was 0.5mV/sec. Cyclic potentiodynamic polarization tests were performed in pure deionized water, lithium hydroxide (LiOH) solutions, and mixtures of lithium hydroxide and boric acid (LiOH + H_3BO_3). Typically about 700 ml of water or solution was added to the cell before each test. All electrochemical measurements were measured at room temperature and open to atmosphere.

The surface of the formed oxides on the alloy was examined by SEM, JEOL JSM 5400.

Results and Discussion

Determination of Corrosion Rate of Zircaloy-4 (Zr-4)

Using Faraday's Law, we can convert the results of electrochemical measurements (I_{corr}, $\mu A/cm^2$) to rates of uniform corrosion (CR, mm/yr) (ASTM, 1994).

$$\text{Corrosion Rate (CR)} = \frac{\text{K}.\, I_{corr}\,.\, \text{EW}}{\rho}$$

Corrosion Rate (CR), mmpy
K (constant) = 3.27×10^{-3}), mm.g/(μA.cm.yr)
Corrosion Current Density (I_{corr}), μA/cm^2
Equivalent Weight (EW) = atomic weight of the metal/valence
Density of the metal (ρ), g/cm^3

For alloys, the equivalent weight is more complex. The alloy equivalent weight, EW, is the reciprocal of the total number of equivalents of all alloying elements (ASTM, 1994).

$$\text{EW}_{\text{alloy}} = \frac{1}{\text{N}_{\text{eq}}}$$

$$\text{Neq} = \Sigma \frac{\text{fini}}{\text{Wi}}$$

Where:
fi = the mass fraction of the i element in the alloy
ni = the valence of the i element of the alloy
Wi = the atomic weight of the i element in the alloy

Normally alloying elements at concentrations below 1% (Table 1) by mass were not included in the calculation, for example, they were considered part of the basis metal (ASTM, 1994).

Mass fraction of zirconium (Zr) = 95.5%
Mass fraction of tin (Sn) = 1.5%
Standard atomic weight of zirconium element = **91.224** U
Valence of zirconium = 4
Standard atomic weight of tin element = **118.710** U
Tin has two variable valences (^{50}Sn: [Kr] $4d^{10}$ $5s^2$ $5p^2$) = 2 and 4
Equivalent Weight of Zr-4 = 23.018 U
Density of Zircaloy-4 at room temperature = 6.58 g/cc (IAEA, 2008)

$$\boxed{\text{Corrosion Rate (mmpy)} = \frac{0.00327 \times 23.018 \times I_{corr}\,(\mu A/cm^2)}{6.58}}$$

Effect of Lithium Hydroxide (LiOH) on the Corrosion Rate

During the corrosion of zirconium alloys in aqueous environments an oxide film isolates the alloy from the environment. Oxidation of Zircaloy occurs by electrochemical reactions at the surface; Oxidation of zirconium metal to zirconium oxide is the anodic reaction responsible for the degradation of the cladding wall. Reduction of water to either atomic hydrogen or hydrogen gas is the cathodic reaction (Weidinger et al., 1991). A net reaction is: $Zr + 2H_2O \rightarrow ZrO_2 + 2H_2$.

A review of waterside corrosion data, including information available in the presented work as well as unpublished data in Master’s degree study. It was found that the Zr-4 waterside corrosion closely follows the zirconium and Zr-2 corrosion at room temperature and increasing corrosion resistance to lithiated solutions in the order Zr > Zr-4 > Zr-2.

As presented in Table 1, there is no simple relationship between LiOH concentration and corrosion rate, the corrosion rate is slightly increased by increasing Li ions concentration in the coolant with respect to pure water. It was found the corrosion current density is 0.8159μA/cm^2 at 100 ppm Li ions. This slight effect of the lithium hydroxide on the corrosion rate can be due to a PH effect. Based on SEM analyses, oxide films formed in diluted lithiated solutions maintain their integrity until concentration of Li ions in water reaches 30 ppm, so very dilute solutions probably have no effect on oxide surface topography.

At very high LiOH concentrations ≥ 0.5 M, there is very high corrosion rate, is greater than what can be accounted for by its PH effect. Therefore, the cause of accelerated corrosion at high lithium concentrations can be related to a combined effect of PH and LiOH since the tests performed with KOH instead of LiOH (at equivalent coolant PH) lead to no significant acceleration of the corrosion rate (Pêcheur et al., 1996) and (Pêcheur et al., 1993). Since the cationic species in the coolant appears to have a significant influence on the oxidation process. In another area to seek evidence for the effect of lithium on the corrosion of zircaloy, other alkalis have only minor and decreasing effects in the order LiOH > NaOH > KOH > NH_4OH (Coriou et al., 1962). Furthermore, no other salt of lithium apparently has any effect on zirconium alloy corrosion. Moreover, no effects are observed in fused LiOH (Ramasubramanian, 1980). Since the anionic and cationic species in the coolant appears to have a significant influence on the oxidation process. Thus, the phenomenon is neither an effect of PH, $[OH^-]$, nor of Li^+ but is a unique property of LiOH (Cox et al., 1996).

Moderate concentrations of LiOH solutions that are 0.1 M or less in concentration at room temperature appear capable, at most, only of generating superficial pores in oxide films, from SEM micrographs. By contrast, concentrated solutions of LiOH, 0.5 M or more, can generate pores cover the whole surface and passes through the whole oxide film reaching to alloy-oxide interface and largely increases the corrosion rate within these short-duration tests (highly porous oxides meaning non protective). This conclusion stems mainly from the high corrosion rate determined by Tafel calculations because the corrosion rate depends on the diffusion of oxygen or oxidant species through the inner barrier layer (impervious layer) (Garzarolli et al., 1982) and (Baur et al., 2000) and any increasing of the oxygen ion diffusion, which in turn increases the corrosion rate. Therefore one of the possible influences of the LiOH could be upon the oxygen transport across the oxide film.

From Tafel calculations, the corrosion rate was accelerated at 3500 and 7000 ppm Li, equals 368.68×10^{-3} and 69.572×10^{-3} mm/y, respectively (Table 1). So the values 0.5 to 1 M LiOH at room temperature are a critical concentration values for accelerated corrosion of the fuel cladding, Zr-4. At these critical concentrations (which lie between 0.5 and 1.0 M LiOH for Zircaloy-4 at room temperature), Generation of porosity in the oxide films, which allows easy access of the corrodant to the oxide-alloy interface, which increases the density and hence availability of short-circuit diffusion paths, are generally identified with an increasing corrosion rate. This conclusion is in agreement with results of Sabol and McDonald and others (Sabol et al., 1974) and (Cox, 1976). Therefore, we have concluded that a lithium effect increasing rapidly the corrosion rate, when no boron present, is highly due to porosity generation (Fig. 8). Accelerated corrosion of Zr-4 by porosity generation model was suggested by others (Cox et al., 1996) and (Ramasubramanian, 1991). Below a critical LiOH concentration, only superficial porosity was developed in these short-duration experiments (Fig. 7) and no severe effect of LiOH is observed on the corrosion rate.

Correlation with Autoclaved Tests Data

In autoclaved tests, the corrosion rate is expressed in weight gain unit, mg dm^{-2} d^{-1}. The value of the critical LiOH concentration, where pretransition kinetics disappear and post-tarnsition rate accelerate was determined by many investigators: Kass (Kass, 1969) found Zr-2 has very high corrosion rates with 0.1 to 1 N LiOH. Coriou et al. (Coriou et al., 1962) found Zircaloy corrosion accelerated at 0.04 M LiOH (280 ppm Li) and 0.25 M NaOH (5750 ppm Na) at 360 °C. Hillner and Chirigos (Hillner and Chirigos, 1962) showed that the pretransition corrosion kinetics disappeared between 0.1 and 0.5 M LiOH. McDonald et al. (McDonald et al., 1984) found a very rapid increase in the corrosion rate of Zr-4 at 0.1 M LiOH at 360 °C. By others, Zr-4 corrosion rate increased at > 350 ppm Li and Zr-2.5Nb Pressure Tube at > 60 ppm Li at 360 °C (Ramasubramanian and Balakrishnan, 1994). Cox et al. (Cox et al., 1996) found the value lies between 0.1 and 1.0 M LiOH for Zr-2 at 300°C. However, it would be expected that the precise value of the critical LiOH concentration would depend on temperature and the alloy involved (Cox et al., 1996). Pêcheur et al. reported high post-transition oxidation rate (0.6 µm/d) with 70 ppm Li ions environments and oxidation rate close to (5 µm/d) at $\geq$700 ppm Li ions, while low oxidation rates (<0.3 µm/d) with diluted solutions at 633 K (Pêcheur et al., 1996) and (Pêcheur et al., 2000). In the presented work, the Zr-4 material is electrochemical oxidized, the corrosion rate is expressed in the penetration unit, mmpy, and pre or post-transition kinetics can not be followed, the value of the critical LiOH concentration, where rate of Zr-4 accelerate compared with the corrosion rate in pure water is determined. We found that the corrosion rates are acclereated at 0.5 and 1 M LiOH at room temperature, equals 0.36868 mmpy at 0.5 M LiOH.

The Impact of $[Li]_{coolant}$ = 2.2 and 3.5 ppm on Corrosion Rate of Zr-4

The new types of fuel management (longer cycle and high burnup) will require an increase of the boron content in the coolant. It will be necessary to increase the lithium content in the fluid to PH control. An attempt is made using the CEA corrosion model (COCHISE) to determine the influence of increasing the lithium content in the primary coolant of PWRs in France (with lithium content, usual 2.2 and elevated 3.5 ppm early in the cycle) on fuel cladding corrosion. The measurements led to a calculated increase in the corrosion data of around 30% due to Li increasing in coolant (Billot et al., 1994). A simple electrochemical experiment in this work used for the impact of 3.5 ppm Li ions in the water on the corrosion rate. From the data in Table 3 and cyclic polarization curves for published and unpublished data (Fig. 10-11), it was clear that the corrosion rate at 2.2 ppm Li ions in water less than those of pure water. Increasing lithium ions content in the water (3.5 ppm) led to the observation of a non-negligible increase in corrosion rates than H_2O and 2.2 ppm Li ions. In addition, localized corrosion due to positive hysteresis loop was observed at 3.5 ppm for zirconium and Zr-4 (Fig. 2 and 10), this increases the corrosion rates.

Effect of Boric Acid on the Corrosion Rate

It has been confirmed experimentally that the presence of boric acid in the coolant slows down Zircaloy corrosion rate (Billot et al., 1994). In our study, in LiOH solution containing 100 ppm of lithium, the presence of as low as 10 ppm of boron was found to decrease the corrosion rate (Table 1). The ameliorating effect of boron increase with increasing concentration of the boric acid, therefore, neutralizing action can be concluded (i.e. lowers the PH of the solution). This observation is consistent with Perkins and Busch and other investigators (Perkins and Busch, 1991). SEM analyses have shown that the porosity generated by lithium hydroxide completely blocked in presence of 1000 ppm B (Fig. 9). Therefore, boron could form a protective film preventing oxidizing species from entering the oxide film. It is proposed that boron, existing in the coolant as H_3BO_3 and $H_4BO_4^-$, functions as a blocking agent (Billot et al., 2002). And/or Formation of complex lithium zirconate borate ($Li_xZr_yB_zO_n$), that can plug the pores result in suppression the ingress of lithium into the inner layer (Cox et al., 1996). No additive analyses for these features were performed. Another mechanism for the ameliorating effect of boron, added as boric acid by interfering with the reaction between LiOH and anion vacancies to prevent the formation of surface OLi groups which could impede the normal growth of oxide crystallites (Ramasubramanian and Balakrishnan, 1994). In contrast, experiments conducted by Bramwell et al, In solutions containing 220 ppm of lithium, the presence of as little as 50 ppm of boron had a marked ameliorating effect on the corrosion rates of Zircaloy-4. But experiments with the same lithium concentration but just 10 ppm of boron resulted in consistently higher weight gains than in the lithium-only test, suggesting that the concentration of boron must exceed a certain critical value before corrosion can be inhibited, and that concentrations below this threshold increase corrosion rates. It must be expected that the threshold boron concentration will be a function of the lithium concentration and temperature, (Bramwell et al., 1991). Similar to acceleration of corrosion by lithium, the inhibition by boron can be related to a combined effect of PH and H_3BO_3.

We take in consideration two important items:

1- Erratic results (i.e., a small decrease and a slight increase in corrosion rate are seen) for the Zr-4 and (Zr-2, and zirconium, unpublished data). These erratic observations have also been reported by others in autoclaved tests (Ramasubramanian and Balakrishnan, 1994), (Billot et al., 1994), and (Manolescu et al., 1982). The decrease in corrosion rate with increase in lithium is significant, however, is not understood. In fact, there is no simple relationship between PH (LiOH) and corrosion. In addition, the effect of lithium hydroxide on the oxidation rates seems to depend not only on the water chemistry (LiOH and H_3BO_3 concentrations) but also on the characteristics of the inner barrier layer.

2- Temperature consideration, in high temperature the critical value is expected to appear at concentration less than 0.5 M LiOH according to Arrehenius-equation where corrosion rate depends on reaction temperature or alloy-oxide interface temperature. Moreover, it is known from isothermal tests that there is a synergism between temperature and lithium hydroxide concentration in affecting the corrosion of Zircaloy-4 (McDonald et al., 1984). In addition, the dissociation of LiOH, decreases with increase in the temperature, undissociated LiOH is expected to impede the recrystallization and normal growth of oxide crystallites and thus maintain a high intercrystalline grain boundary area for oxygen diffusion to occur (Ramasubramanian and Balakrishnan, 1994).

Cyclic Potentiodynamic Polarization Curves

Figure 1 shows a cyclic polarization graph of Zr-4 was corroded in Pure Water at room temperature. The cyclic polarization curve shows the largest potential region over which the specimen remains passive in water than the other solutions. Similar curves were also obtained in 2.2, 5, 10, 30, 50, 70 ppm Li ions, but take in consideration, the passive zone decreases with increase the Li ions concentration. The more extended the passive region, the better the resistance to localized corrosion and the better the passivation characteristics (Klar and Samal, 2007). The loop is on the left (negative hysteresis) as in the reverse anodic scan the current density was less than that for the forward scan, indicating no localized corrosion susceptibility of Zircaloy-4 sample. The Zr-4 material exhibited an increase in current at potential above 1.3 V or higher. This is associated with the oxidation of water to form oxygen rather than with breakdown of the oxide (Marek et al., 2005).

Figure 2 shows a cyclic polarization graph of Zr-4 was corroded in 3.5 ppm Li as LiOH.H2O at room temperature. The polarization curve exhibited oxide breakdown, which in this case critical pitting potential (E_{pit}) was occurred at potential less than 0.8 V. The loop is on the right (positive hysteresis), indicating localized susceptibility of Zircaloy-4 sample at this concentration of lithium (3.5 ppm) (the appearance of localized corrosion, to the knowledge of the authors, has not been previously reported, and can be one of the causes of increasing corrosion of Z-4 after new fuel management, increasing Li ions to 3.5 ppm). This means Zr-4 undergoes localized corrosion in addition uniform corrosion. The smaller the area under the hysteresis loop indicates the smaller the amount of localized corrosion incurred by the material. The protection or the repassivation potential (E_p or E_{rep}), the potential at which the reverse scan intersects the forward scan, was reported at ~ 0.25 V and is more negative (cathodic) than the pitting potential indicating pitting could occur. Between the pitting potential and protection potential, $E_{pro} < E < E_{pit}$, new pits will not form, but existing ones will propagate (Bertolini et al., 2013).

Figure 3 shows a cyclic polarization graph of Zr-4 was corroded in 100 ppm Li as LiOH.H2O at room temperature. The cyclic polarization curve shows the breakdown of passivity phenomenon of Zircaloy-4 sample at 100 ppm Li against the uniform corrosion. The passive zone was reduced, and the breakdown potential (E_{bd}) appeared as 700 mV. The loop is on the left (negative hysteresis), indicating the passive film formed on the surface of the specimen is protective and self-healing (Darabara et al., 2004). In other words, negative hysteresis indicates that the damaged passive film repairs itself (Tait, 1994).

Figure 4 shows a cyclic polarization graph of Zr-4 was corroded in 7000 ppm Li (1M LiOH) as $LiOH.H_2O$ at room temperature. The cyclic polarization curve shows the unability of the Zr-4 to spontaneously passivate in the 1M LiOH medium. The region around the vertex value indicates an unstable passivating system. The breakdown potential at 0.5 V, and passive zone was quasi-disappearance. The resistance to corrosion of an alloy increases with an increase in the breakdown potential (E_b), passive region (ΔE_p), and repassivation potential (E_{rep}) (Kim, 2011). The corrosion resistance of Zr-4 decreases with increase the LiOH concentration due to the decrease in protectiveness of the passive layer. The curve shows that, LiOH is able to instigate the breakdown of the oxide passivity and change properties of the barrier layer (thickness and protectiveness).

Figure 5 shows a cyclic polarization graph of Zr-4 was corroded in 100 ppm Li as LiOH.H2O + 4000 ppm B as H_3BO_3 at room temperature. The cyclic polarization curve shows that, boron added as boric acid abates the effect of lithium hydroxide. Similar curve for corrosion of Zr-4 in pure H2O was obtained.

Conclusion

1- Zircaloy-4, in absence of boric acid, is largely electrochemical corroded at high lithium concentration. The levels of LiOH used in pressurized water reactors (PWR) are much below the amounts needed to cause accelerated corrosion in these electrochemical tests. But take in consideration, susceptibility of Zr-4 to localized corrosion at 3.5 ppm Li from cyclic potentiodynamic polarization curve.

2. Below some critical LiOH concentration, which is a function of alloy and temperature, only superficial pores can be generated and the effect of LiOH is limited. At these critical concentrations, corrosion films were very porous and oxidation kinetic is accelerated.

3. For Zircaloy-4 at room temperature, this critical concentration lies between 0.5 and 1.0 M (3500 and 7000 ppm Li).

4. In solutions containing 100 ppm of lithium ions, the presence of as little as 10 ppm of boron slows down Zircaloy corrosion rates at room temperature. The decrease in corrosion rates appear to be proportional to the boron content in the fluid, hence, PH effect can be concluded. SEM imaging suggests that the plugging of pores occurs by boric acid itself or B/Li complex that result in suppress the ingress of lithium into the inner layer and development of deep pores in the oxide. i. e. the inhibition by boron can be related to a combined effect of PH and H_3BO_3.

TABLE 1–Cladding material chemical composition

Cladding	Nominal Composition			
Zr-4	Zr	1.5% Sn	0.2% Fe	0.1% Cr

Table 2: Rate of Corrosion of Zircaloy-4

Medium	I_{corr} ($\mu A/cm^2$)	Corrosion Rate (mmpy)
Pure deionized water	0.1098	$1.256006205 \times 10^{-3}$
2.2 ppm Li	0.03007	$0.3439718268 \times 10^{-3}$
3.5 ppm Li	0.1605	$1.835965354 \times 10^{-3}$

5 ppm Li	0.2266	$2.592085665 \times 10^{-3}$
10 ppm Li	0.3299	$3.773738133 \times 10^{-3}$
30 ppm Li	0.07595	$0.8687948202 \times 10^{-3}$
50 ppm Li	0.03832	$0.4383438777 \times 10^{-3}$
70 ppm Li	0.1226	$1.402425872 \times 10^{-3}$
100 ppm Li	0.8159	$9.33109859 \times 10^{-3}$
350 ppm Li	0.6449	$7.377034622 \times 10^{-3}$
700 ppm Li	0.1172	$1.340655075 \times 10^{-3}$
3500 ppm Li	32.23	**$368.680145 \times 10^{-3}$**
7000 ppm Li	6.082	**69.572219×10^{-3}**
100ppm Li + 10ppm B	0.4247	$4.858158791 \times 10^{-3}$
100ppm Li + 50ppm B	0.4418	$5.053766314 \times 10^{-3}$
100ppm Li + 100ppm B	0.2061	$2.357585417 \times 10^{-3}$
100ppm Li + 1000ppm B	0.03191	$0.3650196539 \times 10^{-3}$
100ppm Li + 2000ppm B	0.009283	$0.1061885756 \times 10^{-3}$
100ppm Li + 4000ppm B	0.03548	$0.4058570141 \times 10^{-3}$

Table 3: Rate of Corrosion of Zirconium, Zr-2, and Zr-4

Material	Medium	I_{corr} ($\mu A/cm^2$)	Corrosion Rate (mmpy) $\times 10^{-3}$	Type of Hysteresis
Zirconium	Pure H2O	0.06959	0.795968926	negative
	2.2 ppm	0.0001224	1.400008572	negative
	3.5 ppm	0.1273	1.456054667	**Positive hysteresis**
Zircaloy-2	Pure H2O	0.1473	1.692687493	negative
	2.2 ppm	0.1111	1.276697763	negative
	3.5 ppm	0.1586	1.822540641	**negative hysteresis**
Zircaloy-4	Pure H2O	0.1098	1.256006205	negative
	2.2 ppm	0.03007	0.343971827	negative
	3.5 ppm	0.1605	1.835965354	**positive hysteresis**

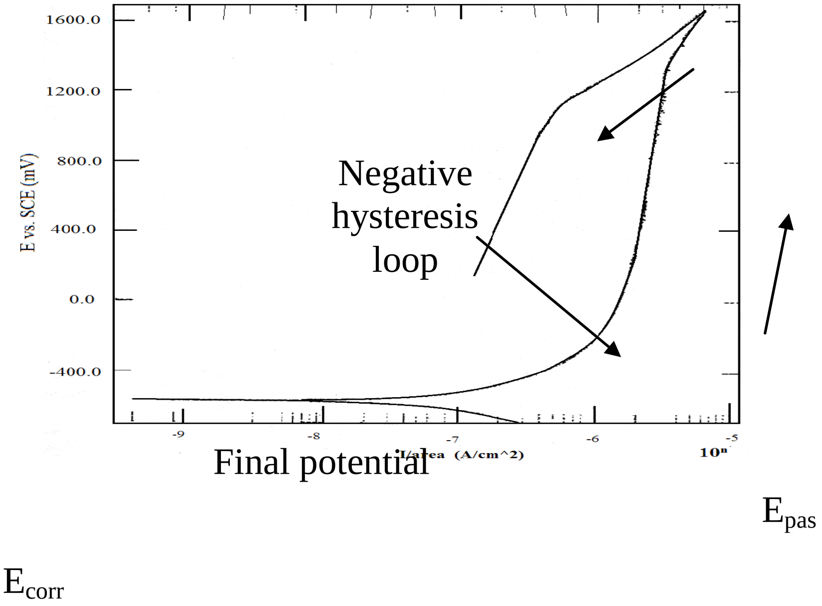

Initial potential

Figure 1: Cyclic Polarization Curve for Zr-4 Corroding in Deionized Pure Water at room temperature

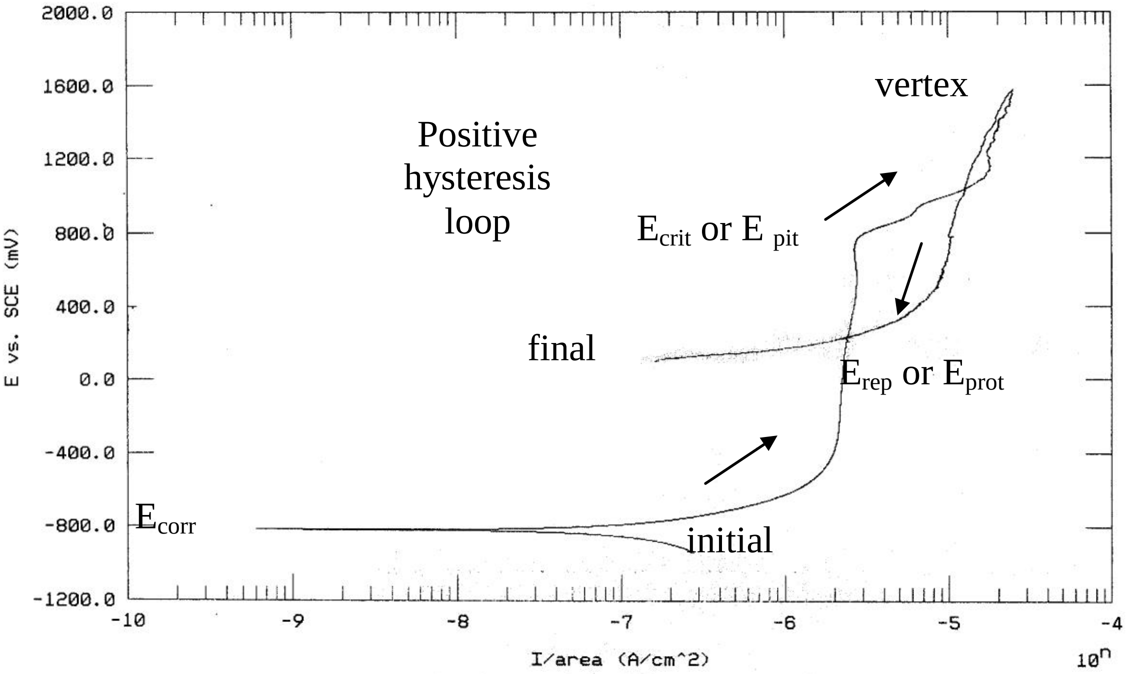

Figure 2: Cyclic Polarization Curve for Zr-4 Corroding in 3.5 ppm Li as $LiOH.H_2O$ at room temperature

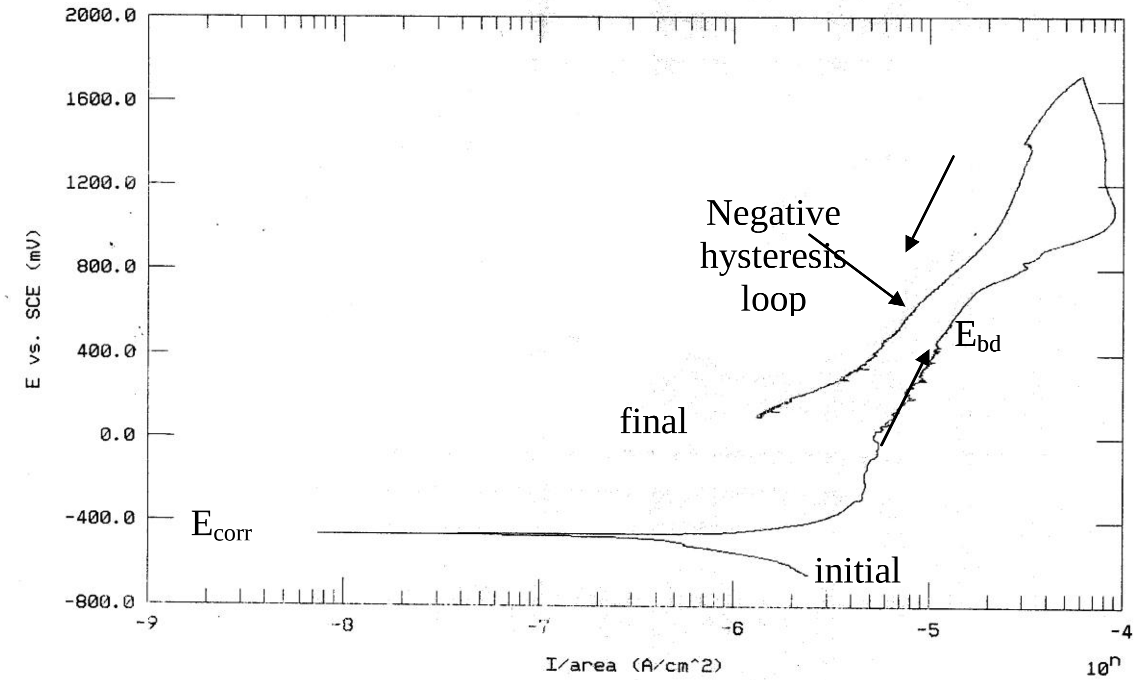

Figure 3: Cyclic Polarization Curve for Zr-4 Corroding in 100 ppm Li as $LiOH.H_2O$ at room temperature

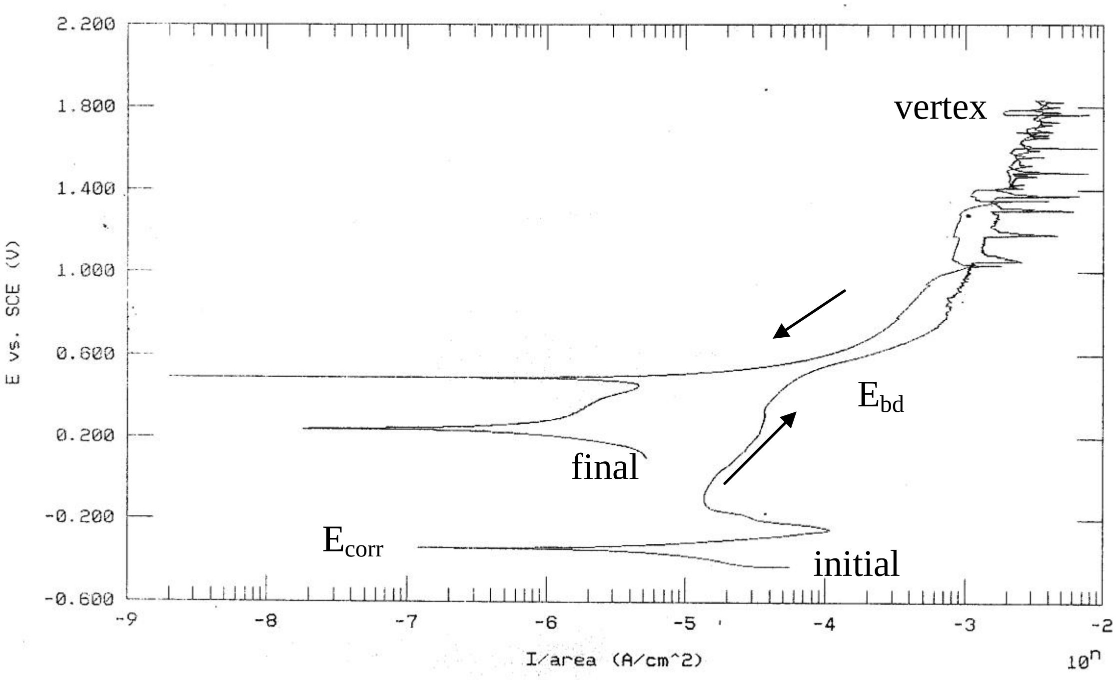

Figure 4: Cyclic Polarization Curve for Zr-4 Corroding in 7000 ppm Li as LiOH.H_2O at room temperature

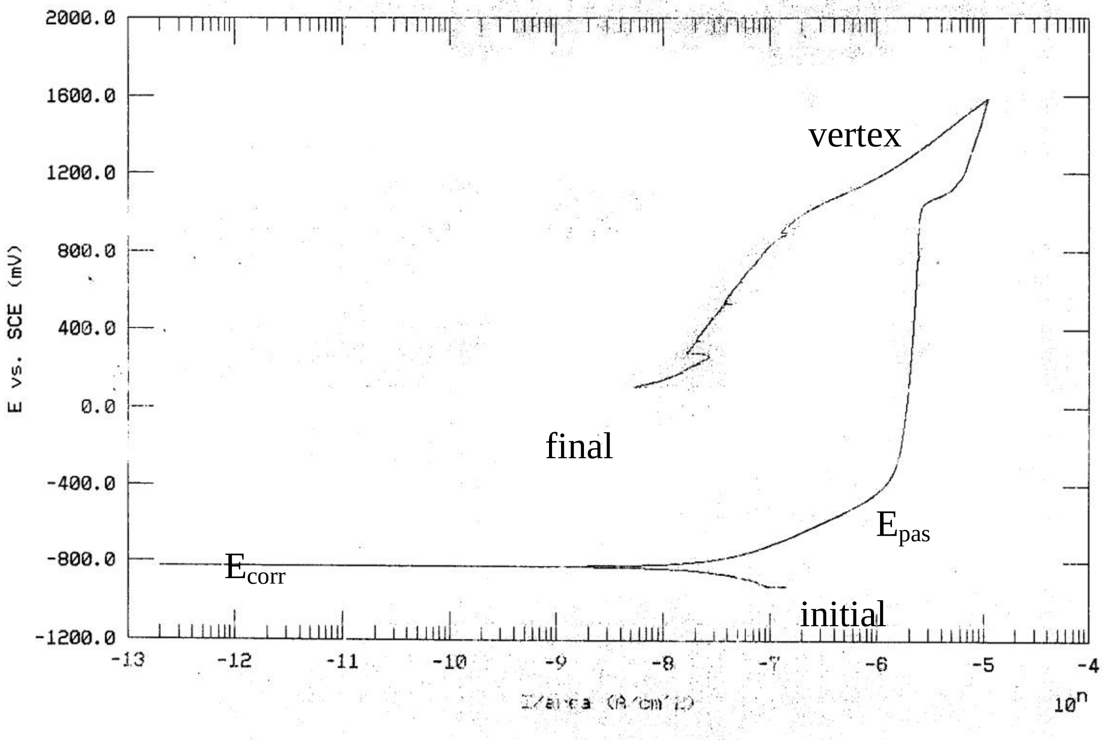

Figure 5: Cyclic Polarization Curve for Zr-4 Corroding in 100 ppm Li as LiOH.H_2O + 4000 ppm B as H_3BO_3 at room temperature

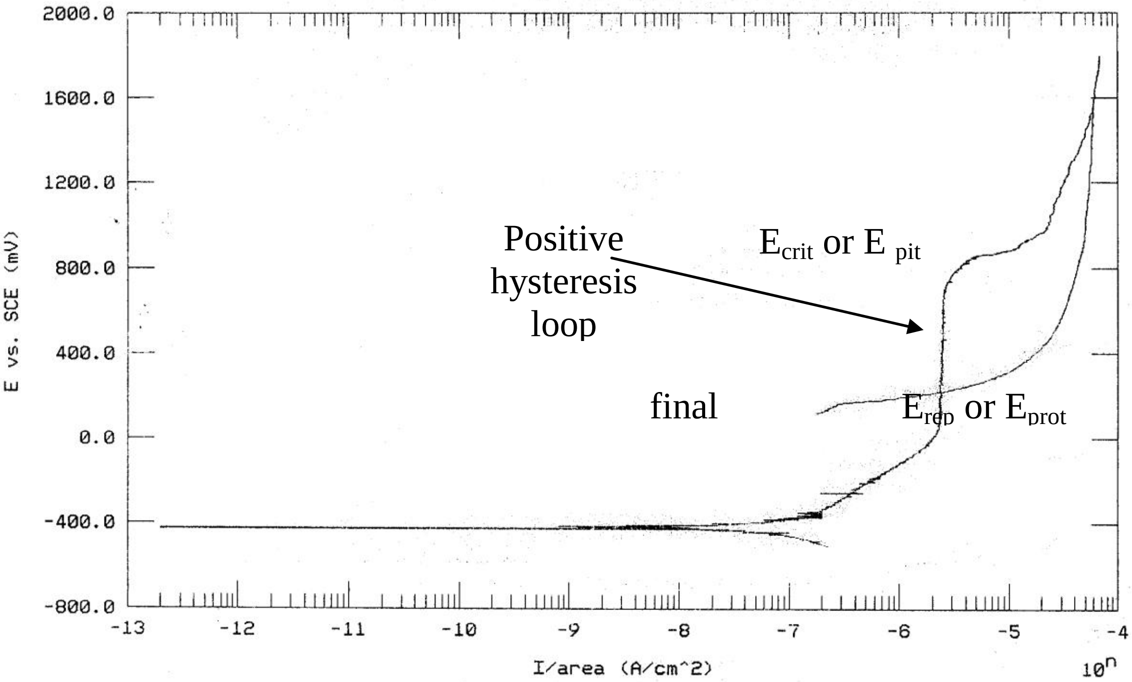

Figure 10: Cyclic Polarization Curve for Zr Corroding in 3.5 ppm Li as LiOH.H_2O at room temperature

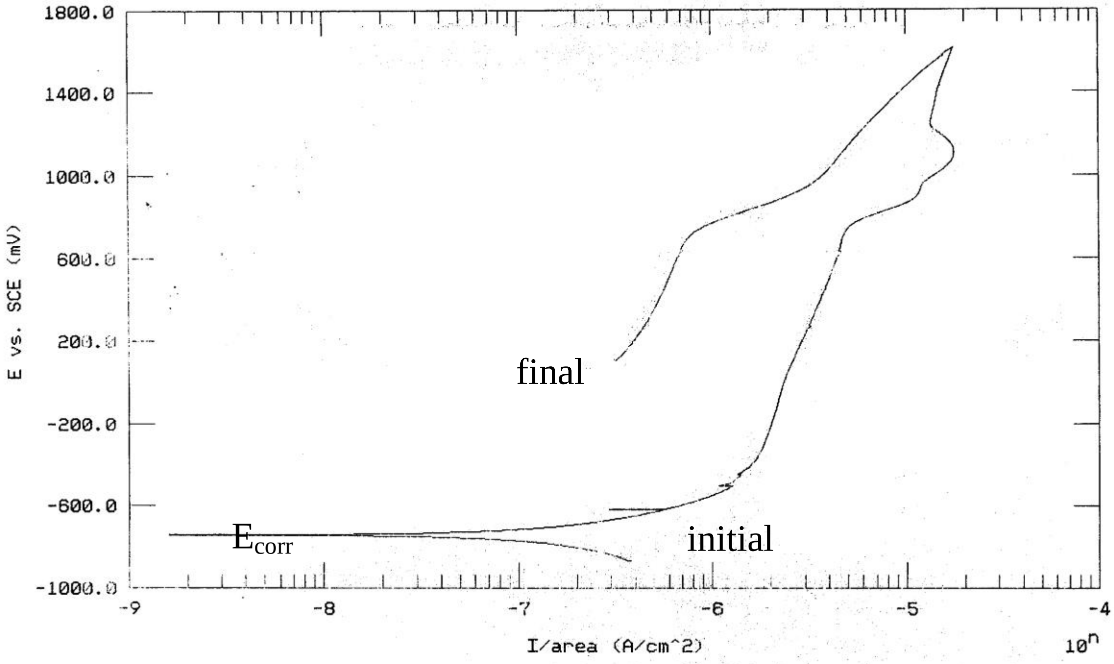

Figure 11: Cyclic Polarization Curve for Zr-2 Corroding in 3.5 ppm Li as LiOH.H_2O at room temperature

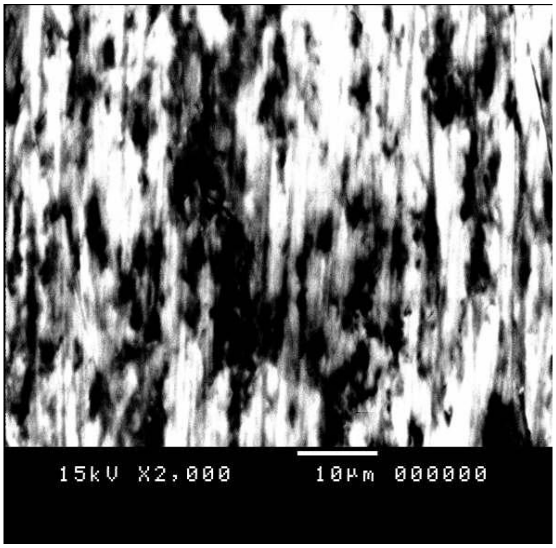

Fig. 6: SEM micrograph of Zr-4 corroded in pure deionized water H_2O

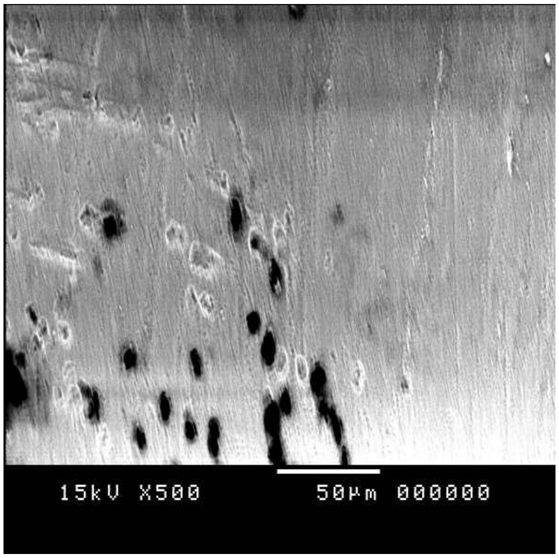

Fig. 7: SEM micrograph of Zr-4 corroded in 100 ppm Li as $LiOH.H_2O$

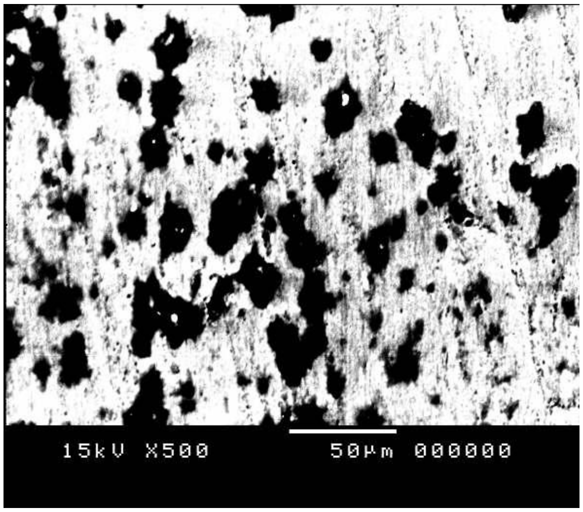

Fig. 8: SEM micrograph of Zi-4 corroded in 7000 ppm Li as $LiOH.H_2O$

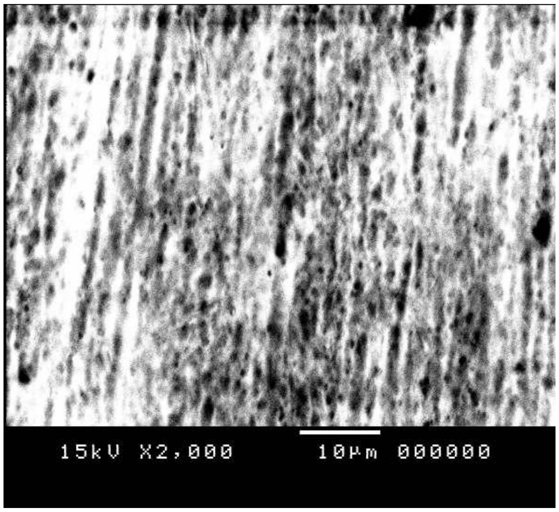

Fig. 9: SEM micrograph of Zr-4 **corroded in 100 ppm Li as $LiOH.H_2O$ + 1000 ppm B as H_3BO_3**

References

ASTM G102, (1994): Standard Practice for Calculation of Corrosion Rates and Related Information from Electrochemical Measurements, pp. 417-419.

Baur, K., Garzarolli, F., Ruhmann, H., and Sell, H.-J. (2000): "Electrochemical Examinations in 350oC Water with Respect to the Mechanism of Corrosion-Hydrogen pickup," Zirconium in the Nuclear Industry: Twelfth International Symposium, ASTM STP 1354, G. P. Sabol and G. D. Moan, Eds., American Society for Testing and Materials, West Conshohocken, PA, pp. 836-852.

Bertolini, L., Elsener, B., Pedeferri, P., Redaelli, E., Polder, R. B.(2013): "Corrosion of Steel in Concrete: Prevention, Diagnosis, Repair Book," Section 7, Electrochemical Aspects.

Billot, P., Yagnik, S., Ramasubramanian, N., Peybernes, J., and Pêcheur, D. (2002): "The role of Lithium and Boron on the Corrosion of Zircaloy-4 Under Demanding PWR-Type Conditions," Zirconium in the Nuclear Industry: Thirteenth International Symposium, ASTM STP 1423, G. D. Moan and P. Rudling, Eds., American Society for Testing and Materials, West Conshohocken, PA, pp. 169–189.

Billot, P., Robin, J.-C., Giordano, A., Peybernes, J., Thomazet, J., and Amanrich, H. (1994): "Experimental and Theoretical Studies of Parameters that Influence Corrosion of Zircaloy-4," Zirconium in the Nuclear Industry: Tenth International Symposium, ASTM STP 1245, A. M. Grade and E. R. Bradley, Eds., American Society for Testing and Materials, Philadelphia, pp. 351–377.

Bramwell, I. L., Parsons, P. D., and Tice, D. R. (1991): "Corrosion of Zircaloy-4 PWR Fuel Cladding in Lithiated and Borated Water Environments," Zirconium in the Nuclear Industry: Ninth International Symposium, ASTM STP 1132, C. M. Eucken and A. M. Grade, Eds., American Society for Testing and Materials, Philadelphia, pp. 628–642.

Cheng, B., Gilmore, P. M., and Klepfer, H. H.(1996): "PWR Zircaloy Fuel Cladding Corrosion Performance, Mechanisms, and Modeling," Zirconium in the Nuclear Industry: Eleventh International Symposium, ASTM STP 1295, E. R. Bradley and G. P. Sabol, Eds., American Society for Testing and Materials, pp. 137-160.

Coriou, H., Grall, L., Meunier, J.,Pelras, M. and Willermoz, H. (1962): Journal of Nuclear Materials, Vol. 7, pp. 320–327.

Cox, B. (1976): in Advances in Corrosion Science and Technology, Vol. 5, M. G. Fontana and R. W. Staehle, Eds., Plenum Press, New York.

Cox, B., Ungurela, M., Wong, Y.-M., and Wu, C. (1996): "Mechanisms of LiOH Degradation and H3BO3 Repair of ZrO_2 Films," Zirconium in the Nuclear Industry: Eleventh International Symposium, ASTM STP 1295, E. R. Bradley and G. P. Sabol, Eds., American Society for Testing and Materials, pp. 114-136.

Darabara, M., Bourithis, L., Zinelis, S., and Papadimitriou, G. D. (2004): "Susceptibility to Localized Corrosion of Stainless Steel and NiTi endodontic Instruments in Irrigating Solutions," International Endodontic Journal, pp. 705-710.

Garzarolli, F., Jorde, D., Manzel, R., Politano, J. R., and Smerd, P. G. (1982): "Waterside Corrosion of Zircaloy-Clad Fuel Rods in a PWR Environment, " Zirconium in the Nuclear Industry: Fifth Conference, ASTM STP 754, D. G. Franklin, Ed., American Society for Testing and Materials, 1982, pp. 430–449.

Garzarolli, F., Jung, W., Shoenfeld, H., Garde, A. M., Parry, G. W., and Smerd, P. G. (Dec. 1982): "Waterside Corrosion of Zircaloy Fuel Rods," EPRI NP-2789, Research Project 1250-1, Kraftwerk Union, AG and Combustion Engineering, Inc., Electric Power Research Institute, Palo Alto, CA.

Garzarolli, F., Seidel, H., Tricot, R., and Gros, J. P. (1991): in Zirconium in the Nuclear Industry: Ninth International Symposium, ASTM STP 1132, C. M. Eucken and A. M. Grade, Eds., American Society for Testing and Materials, West Conshohocken, PA, p. 395–415.

Hillner, E., and Chirigos, J. N. (1962): "The Effect of Lithium Hydroxide and Related Solutions on the Corrosion Rate of Zircaloy in 680^oF Water," Report WAPD-TM-307, Bettis Atomic Power Laboratory, Pittsburgh, PA.

IAEA Publications. (2008): Thermophysical Properties of Materials for Nuclear Engineering: A Tutorial and Collection of Data, Vienna, 2008, P. 149.

Kass, S. (1969): Corrosion, Vol. 25, No. 1, pp. 30-36.

Kim, Y. S., Woo, H. K., Im, K. S., and Kwun, S. I. (2002): “The Cause for Enhanced Corrosion of Zirconium Alloys by Hydrides,” Zirconium in the Nuclear Industry: Thirteenth International Symposium, ASTM STP 1423, G. D. Moan and P. Rudling, Eds., American Society for Testing and Materials, West Conshohocken, PA, pp. 274–296.

Kim, S-Y., Kim, S-T., Lee, I-S., Park, Y-S., Shin, M-C., and Kim Y-S. (2011): “Investigation of the Resistance to Localized Corrosion Associated with Microstructure of Tube-to-Tube Sheet Welds of UNS S32050 Super Austenitic Stainless Steel for Seawater Cooled Condenser,” Japan Institute of Metals, Vol. 52, No. 7, pp. 1388-1395.

Klar, E., and Samal, P. K. (2007): “Powder Metallurgy Stainless Steels: Processing, Microstructures, and Properties book,” Chapter 9, Corrosion Testing and Performance, ASTM, p. 155.

Manolescu, A. V., Mayer, P., and Simpson, C. J., (1982): Corrosion, Vol. 38, No. 1, pp. 23–31.

Marek, M., Pawar, V., Tsai, S., Thomas, R., Sprague, J., Hunter, G., and Salehi, A. (2005): “Electrochemical Characterization of Nitinol in phosphate-Buffered Saline,” Medical Device Materials Part 3, California, USA, p. 203.

McDonald, S. G., Sabol, G. P., and Sheppard, K. D. (1984): “Effect of Lithium Hydroxide on the Corrosion Behavior of Zircaloy-4,” Zirconium in the Nuclear Industry: Sixth International Symposium, ASTM STP 824, American Society for Testing and Materials, Philadelphia, pp 519–530.

Oskarsson, M. (2000): “Study on the Mechanisms for Corrosion and Hydriding of Zircaloy,” Division of Mechanical Metallurgy, Department of Materials Science and Engineering, Royal Institute of Technology SE-100 44 Stockholm, Sweden Stockholm, p. 43.
Pêcheur, D., Giordano, A., Picard, E., and Billot, P.(1993): Proceedings, AIEA Technical Meeting on Influence of Water Chemistry on Fuel Cladding Behaviour, Rez, Czech Republic.

Pêcheur, D., Godlewski, J., Billot, P., and Thomazet, J. (1996): “Microstructure of Oxide Films Formed During the Waterside Corrosion of the Zircaloy-4 Cladding in Lithiated Environment,” Zirconium in the Nuclear Industry: Eleventh International Symposium, ASTM STP 1295, E. R. Bradley and G. P. Sabol, Eds., American Society for Testing and Materials, 1996, pp. 94-113.

Pêcheur, D., Godlewski, J., Peybernes, J., Fayette, L., Noé, M., Frichet, A., Kerrec, O. (2000) “Contribution to the Understanding of the Effect of the Water Chemistry on the Oxidation Kinetics of Zircaloy-4 Cladding,” Zirconium in the Nuclear Industry: Twelfth International Symposium, ASTM STP 1354, G. P. Sabol and G. D. Moan, Eds., American Society for Testing and Materials, West Conshohocken, PA, pp. 793-811.

Perkins, R. A. and Busch, R. A. (1991): “Corrosion of Zircaloy in the Presence of LiOH,” Zirconium in the Nuclear Industry: Ninth International Symposium, ASTM STP 1132, C. M. Eucken and A. M. Grade, Eds., American Society for Testing and Materials, Philadelphia, 1991, pp. 595–612.

Ramasubramanian, N. (1980): Journal of the electrochemical society, Vol. 127, pp. 2566-2572

Ramasubramanian, N., Precoanin, N., and Ling V. C. (1989): “Lithium Uptake and the Accelerated Corrosion of Zirconium Alloys,” Zirconium in the Nuclear Industry: Eight International Symposium, ASTM STP 1023, L. F. P. van Swan and C. M. Eucken, Eds., American Society for Testing and Materials, Philadelphia, pp. 187-201.

Ramasubramanian, N. (1991): “Lithium Uptake and the Corrosion of Zirconium Alloys in Aqueous Lithium Hydroxide Solutions,” Zirconium in the Nuclear Industry: Ninth International Symposium, ASTM STP 1132, C. M. Eucken and A. M. Grade, Eds., American Society for Testing and Materials, Philadelphia, pp. 613-627.

Ramasubramanian, N. and Balakrishnan, P. V. (1994): “Aqueous Chemistry Lithium Hydroxide and Boric Acid and Corrosion of Zircaloy-4 and Zr-2.5Nb Alloys,” Zirconium in the Nuclear Industry: Tenth International Symposium, ASTM STP 1245, A. M. Grade and E. R. Bradley, Eds., American Society for Testing and Materials, Philadelphia, pp. 378-399.

Sabol, G. P. and McDonald, S. G. (1974): “Stress Effects and the Oxidation of Metals”, Proceedings Metallurgical Society of the American Institute of Mining, Metallurgical and Petroleum Engineers, pp. 353–372.

Sabol, G. P., Comstock, R. J., Weiner, R. A., McAtee, K. R., Leech, W. J., Correal-Pulver, O. A., Miller, R. S., and Stanutz, R. N. (April 1994): “In-Reactor Corrosion Performance of ZIRLOTM and Zircaloy-4 and Related Corrosion Modelling,” Proceedings, 1994 International Topical Meeting on LWR Fuel Performance.

Sabol, G. P., Comstock, R. J., Weiner, R. A., Larouere P., and Stanutz, R. N. (1994): “In-Reactor Corrosion Performance of ZIRLO and Zircloy-4,” Zirconium in the Nuclear Industry: Tenth International Symposium, ASTM STP 1245, A. M. Grade and E. R. Bradley, Eds., American Society for Testing and Materials, Philadelphia, pp. 724–744.

Tait, S.W. (1994): An introduction to eletrochemical corrosion testing for practing engineers and scientists, Pair Docs Publications.

Weidinger, H. G., Ruhmann, H., Cheliotis, G., Maguire, M., and Yau, T.-L. (1991): “Corrosion-Electrochemical Properties of Zirconium Intermetallics,” Zirconium in the Nuclear Industry: Ninth International Symposium, ASTM STP 1132, C. M. Eucken and A. M. Grade, Eds., American Society for Testing and Materials, Philadelphia, pp. 499–535.